

Plant Mediated Synthesis of Silver Nanoparticles by Using Dried Stem Powder of *Tinospora Crispa*, And Study of Its Photoluminescence Activity

R.Sarada¹, Dr. V. Jagannadharao¹, Prof B.Shyama Sunder*

¹Department Of Chemistry, Anil Neerukonda Institute of Technology and sciences. Sangivalasa, Visakhapatnam Dt., India-531162.

* Vice Chancellor, Yogi Vemana University, Kadapa, A.P.,India.

ABSTRACT

The *Tinospora Crispa* is an important medicinal plant to synthesize silver Nanoparticles provides environmentally benign and a feasible alternative to the most of the chemical, physical and biological methods. Utilizing the reduced property of *Tinospora Crispa* dried stem powder from 1mM aqueous silver nitrate, the average size of 40nm silver nanoparticles were synthesized at room temperature. The stem powder extracts mixed with silver nitrate showed a gradual change in the color of the extracts from yellow to dark brown. The formation of silver nanoparticles was confirmed by UV-Visible spectrophotometer, X-Ray diffraction (XRD), Fourier transform infrared (FTIR), Energy dispersive spectroscopy (EDAX) and Transmission electron microscopy (TEM). The photoluminescence studies of silver nanoparticles shows that they are efficient fluorescence emitting probes.

KEY WORDS: Silver nanoparticles, *Tinospora Crispa*, Characterization, X-Ray diffraction (XRD), Fourier transform infrared (FTIR), Photoluminescence.

I. INTRODUCTION

In the last decade, the biosynthesis of nanoparticles has received increasing attention due to the growing need to develop eco-friendly technologies in material synthesis. Sastry and co-workers explored the possibility of using microbes and plant materials as nano-factories for the synthesis of nanometals.¹⁻⁶ But in recent years, the biosynthetic method using plant extracts has received more attention than chemical and physical methods that they are extremely expensive and also involve the use of toxic, hazardous chemicals. The biological method using bacteria, algae and fungi to synthesize silver nanoparticles is very slow and elaborative cell culture maintaining process when in comparison with plant extracts. Gardea-Torresdey et al.^{7,8} initially reported the possibility of using plant materials for the synthesis of nano-scale metals. Later, the bioreduction of various metals to nano-sizes of various shapes, capable of meeting the requirements of diverse industrial applications, was extensively studied.

Metal nanoparticles show new physical and chemical properties as they are playing their role as surface atoms. These novel properties have attracted significant attention because of their interesting optical and electronic

properties, which have resulted in the exploitation of a number of applications in chemistry and in biochemistry.⁹⁻¹⁴ Particularly, the resonance Plasmon effect in photo physical properties of organic chromophores like dyes is still an intricate phenomenon.¹⁵ The optical properties are highly influenced by the preparation methods and conditions, which result in particles of various sizes, shape and surface stabilization. The type, size and shape of the nanoparticles can modulate the fluorescence of a target dye close to the metal surface. The enhancement of the fluorescence efficiency due to the electronic coupling of the electronic transition dipole moment with surface plasmons is a desired effect owing the use of medium to low-quantum yield fluorophores in molecular probing devices.¹⁶⁻¹⁹ In the present study it was demonstrated the ability of biosynthesized silver nanoparticles (Ag-NPs) from warm water extractions of *Tinospora crispa* stem extracts to use as fluorescence emitting probes. The synthesized silver nanoparticles were characterized using UV-Visible spectrophotometer, XRD, FTIR, EDAX and TEM.

II. MATERIALS AND METHODS

2.1 Preparation of *Tinospora crispa*'s stems powder

Fresh *Tinospora crispa* plants were collected from surroundings of Aaraku agency of Visakhapatnam district, Andhra Pradesh, India. Finely cut stems are dried in hot air oven at 50⁰ C to 55⁰ C for one week and then powdered. 100g of *Tinospora crispa*'s dried stem powder was taken in a flask to it 200ml of distilled water was added, then boiled the mixture for 15-20 min and cooled. This cooled mixture was centrifuged at 5000 rpm for 10 min. and collected yellow supernatant. This supernatant is used for further experiments.

2.2 Synthesis of silver nanoparticles

Silver nitrate (AgNO₃) was purchased from Himedia chemicals. In the synthesis of silver nanoparticles, 40ml supernatant of boiled stem powder was added to the 200ml of 1mM of silver nitrate solution and stirred at room temperature. The bio-reduced

component was monitored by using UV-Visible spectrophotometer periodically.

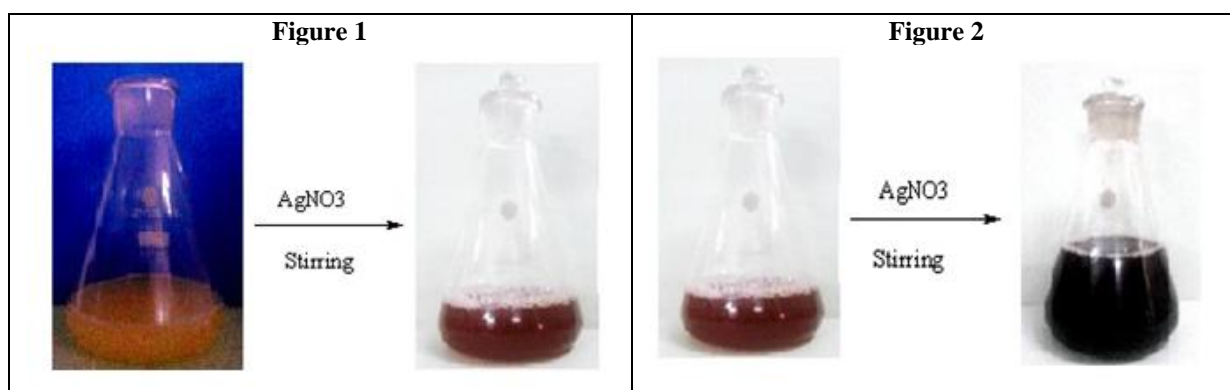
III. RESULTS AND DISCUSSION

3.1 Characterization of silver nanoparticles (Ag NPs)

The presence of Ag NPs was checked by the following methods. These methods provided the evidence that the reaction between silver nitrate and plant's stem powder producing Ag NPs.

3.1.1 Color change

There is a sequential color change which indicates the formation of Ag NPs by our plant material. This is the primary test for the checking of formation of Ag NPs.



Color was changed from yellow to light brown (Fig. 1) and After 18-24hrs color was changed into dark brown (Fig. 2)

The color reduction of AgNO₃ into Nanoparticles was visibly evident from the color change when Stem powder was added into a silver nitrate solution. Within few minutes the appearance of brown color was observed that it indicates the formation of Ag NPs. The color was changed from yellow to light brown (Fig. 1). After 18-24hrs color was changed into dark brown (Fig. 2).

3.1.2 UV-Visible spectral analysis

Synthesized silver nanoparticles was confirmed by sampling the aqueous component of at different time intervals and the absorption maxima was scanned by UV-Visible Spectro-photometer at the wavelength of 300-700 nm on UV-Visible spectrophotometer (Schimadzu UV-Visible spectrophotometer), by using deionized water as the reference.

Figure 3 shows the UV-Visible spectra of silver colloid obtained. The surface Plasmon resonance (SPR) band is broad indicating poly-dispersed nanoparticles. A smooth and narrow absorption band at 443 nm is observed which is characteristic of mono-dispersed spherical nanoparticles. UV-visible spectroscopy is one of the most widely used techniques for structural characterization of silver nanoparticles. The surface

plasmon resonance (SPR) band (λ max) around 443 nm broadened and slightly moved to the long wavelength region, indicating the presence and formation of silver nanoparticles. The optical absorption spectra of metal nanoparticles are dominated by surface Plasmon resonances (SPR), which shift to longer wavelengths with increasing particle size. The position and shape of plasmon absorption of silver nanoclusters are strongly dependent on the particle size, dielectric medium, and surface-adsorbed species. The surface plasmon absorption of silver nanoparticles have the short wavelength band in the visible region around 443 nm is due to the transverse electronic oscillation.

3.1.3 Transmission electron microscopic examination (TEM)

Transmission electron microscopic examination was done to know the morphology of silver nanoparticles, using high-resolution analytical transmission electron microscope (Phillips, Netherland Model: Technai20). In this examination we used centrifuged powder of the solution of silver nanoparticles. For TEM analysis, the specimen was suspended in distilled water, dispersed ultrasonically to separate individual particles, and one or two drop of the suspension

deposited onto holey-carbon coated copper grids and dried under Infrared lamp.

The TEM images obtained for colloid is shown in figure 4. It is clear from the TEM images in figure 4 that the particle size nearly spherical particles of average size 40 nm are obtained. The TEM image confirms the particles are spherical in shape.

The Scherrer rings, characteristic of fcc silver is clearly observed, showing that the structure seen in the TEM image are nano crystalline in nature. It is observed that the silver nanoparticles are scattered over the surface and no aggregates are noticed under TEM. The difference in size is possibly due to the fact that the nanoparticles are being formed at different times.

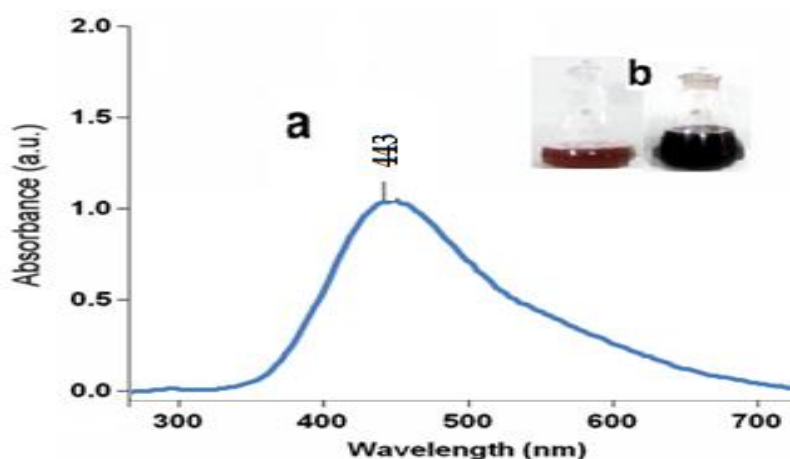


Figure 3: (a) UV-visual absorption spectra of silver nanoparticles after 24 h of reaction. (b) Picture of flask containing the solution of aqueous *Tinospora crispa* stem extract filtrate with silver nitrate in Erlenmeyer flask, before reaction (flask 1) and after 24 h of reaction (flask 2).

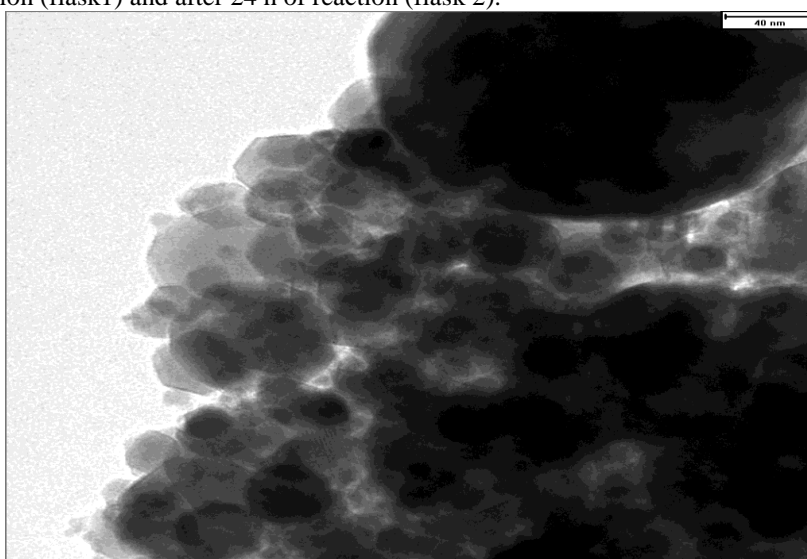


Figure 4: Transmission electron micrographs of the silver nanoparticles used in this work. (a) The bar marker represents 40 nm.

3.1.3 X-Ray diffraction studies (XRD)

The synthesized silver nanoparticles were centrifuged at 10,000 rpm for 15 min. and collected the pellet. The pellet was washed with distilled water to remove impurities and dried to get the powder. The X-Ray diffraction assay was performed for the detection of crystalline nature of the metal nanoparticles was done by X-Ray diffractometer (XPERT-PRO), operating at 40 kV and current of 30mA with Cu K α radiation ($\lambda = 1.5404^\circ$) and the 2θ scanning range was 0-90 $^\circ$ at

2 $^\circ$ min $^{-1}$. The colloidal suspension containing metal nanoparticles was dried on a small glass slab.

Figure 5 shows the XRD pattern of silver nanoparticles obtained using *Tinospora crispa*. The diffraction peaks appeared at 22.41, 23.84, 25.20, 39.11, 42.56, 46.48, and 59.60. The average crystallite size according to Scherrer equation calculated using the highest peak of the 39.11 is found to be 37.36 nm, nearly in agreement with the particle size obtained from TEM image.

3.1.4 Fourier transforms infrared spectroscopy (FT-IR)

To identify the bio-molecules associated with the synthesis of nanoparticles by plant mediated was performed by using FT-IR (Schimadzu FTIR). The dried silver Nanoparticles were grinded and the powder as KBr pellets measured at the wavelength range from 4000 to 400 cm^{-1} .

FTIR measurement was carried out to identify the possible biomolecules responsible for capping and efficient stabilization of silver nanoparticles

synthesized by using *Tinospora crispa*. Figure-6 shows the FTIR spectrum of silver nanoparticles obtained in this study. In the IR spectrum of *Tinospora crispa* capped silver nanoparticles, the spectrum showed absorptions at 3442.90 (OH), at 1597 due to C=O of -COOH, respectively. The band observed at 1357 cm^{-1} is due to C-O stretching mode. The very strong band at 1072 cm^{-1} arises from C-O-C symmetric stretching and C-O-H bending vibrations of protein in the *Tinospora crispa*.

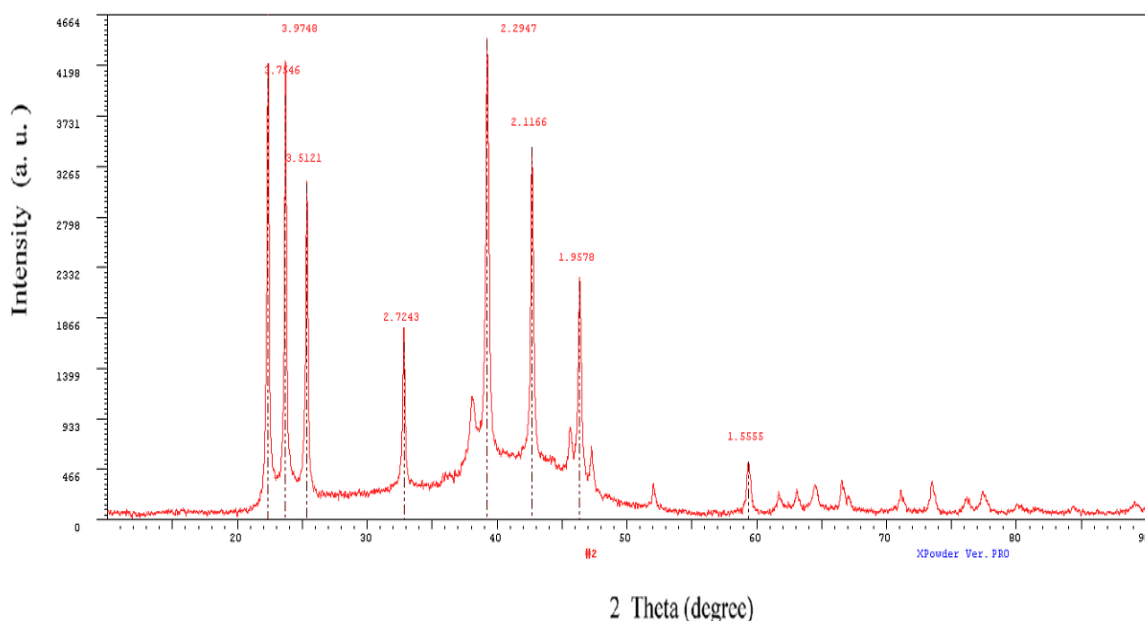


Figure 5: X-ray diffraction pattern of Ag-NP at room temperature synthesized by *Tinospora crispa* stem extract with AgNO_3 solution.

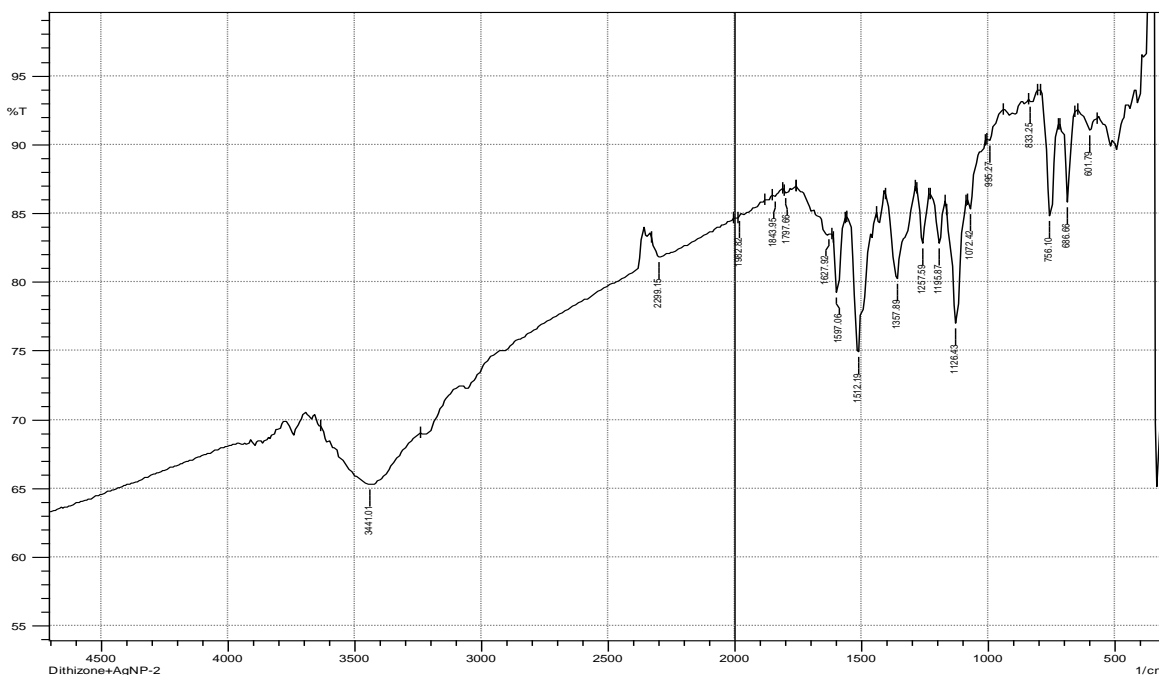


Figure 6: FT-IR spectra of *Tinospora crispa* mediated silver nanoparticles.

Photo physical properties of Ag-NPs & Fluorescein dye in ammonia solution:

The above synthesized Ag-NPs (0.1mmoles) were dissolved in ammonia solution to study their photoluminescence activity. Further these nanoparticles were used in the study of metal enhanced fluorescence (MEF) study.

Fluorescein has been used to derivatize biomolecules for decades, fluorescein-based dyes and their conjugates have several significant drawbacks, including: a relatively high rate of photobleaching, pH-sensitive fluorescence ($pK_a \sim 6.4$), which results in limiting their utility in some multicolor applications, A relatively broad fluorescence emission spectrum shows a tendency toward quenching of their fluorescence on conjugation to biopolymers, particularly at high degrees of labeling. Fluorescein's high photobleaching rate limits the sensitivity that can be observed, a significant disadvantage for applications requiring ultrasensitive detection, such as DNA sequencing, fluorescence *in situ* hybridization and localization of low-abundance receptors. These limitations have encouraged us in the development of new alternative nano fluorophores.

Figure 7 shows the luminescence of Ag-NPs (0.01 % w/v) in ammonia solution at (a) daylight and (b) UV-lamp of 254 nm excitations respectively. Basing on this in view, fluorescence studies were carried on this Ag-NPs. Figure.8 represents the emission spectra of Ag-NPs in ammonia solution at 438 nm. From absorption and emission spectra's the stokes shifts observed as 96 nm. The detailed description with Stokes shifts were compared with emission spectra of flourescein in ammonia solution in figure 9 and the observations were presented in table-1.

Figure 10 display a typical EEMs of Ag-NPs in ammonia. Peak locations and suggested fluorophores are provided in Table 2. The scales of the EEMs listed are not consistent. The purpose of the following discussion is to identify *location* of fluorescent centers and compare those locations with previously identified peaks and their represented fluorophores.

The excitation range (300-500nm) and step interval (5nm) resulted in 41 excitation wavelength data points (300nm, 305nm, 310nm.... 500nm). Emission range (350-700nm) and step interval (5nm) resulted in 70 emission wavelength data points. Following the creation of EEMs, they were then exported into Excel files and later Sigma Plot files and MATLAB files for further interpretation and modeling. From the EEMs spectra location of the peak maxima was found to be: Ex. 342 nm/ Em 438nm, Fluorescence intensity in Raman units.

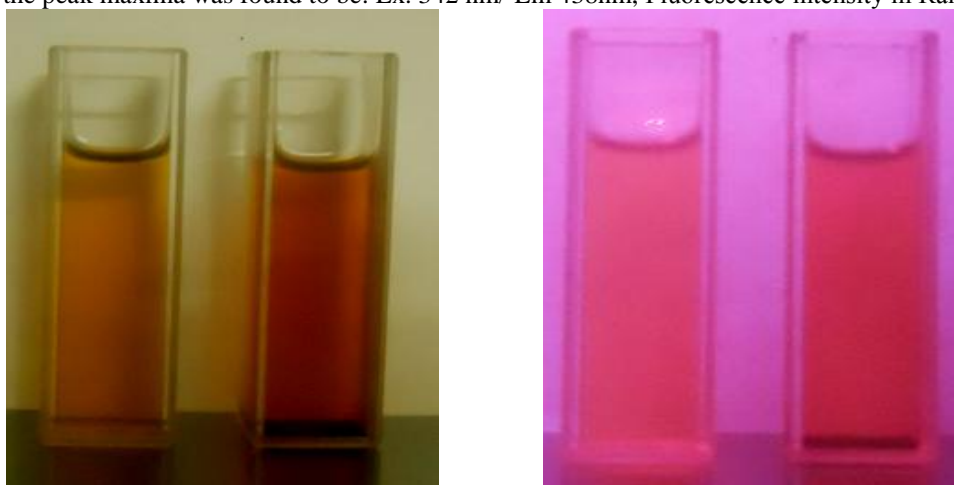


Figure 7: The photos show the luminescence of Fluorescein (Left) & Ag-NP (Right) in ammonia solution @ (a) daylight and (b) 254 nm excitations respectively

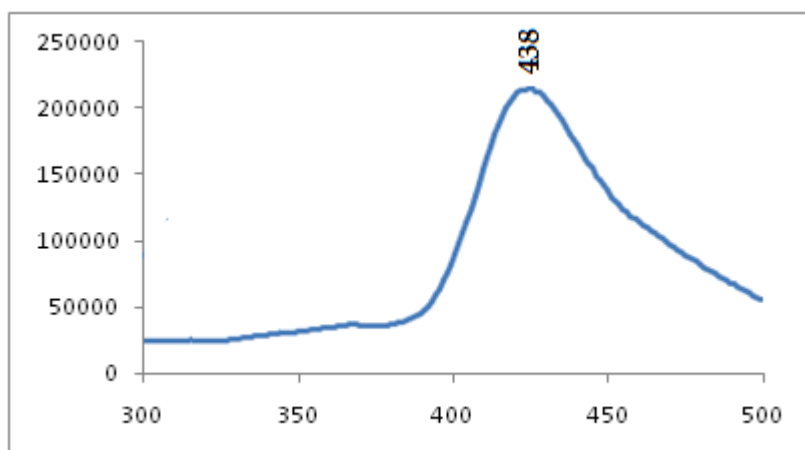


Figure 8: Fluorescence emission of Ag-NP in ammonia at 342nm excitation.

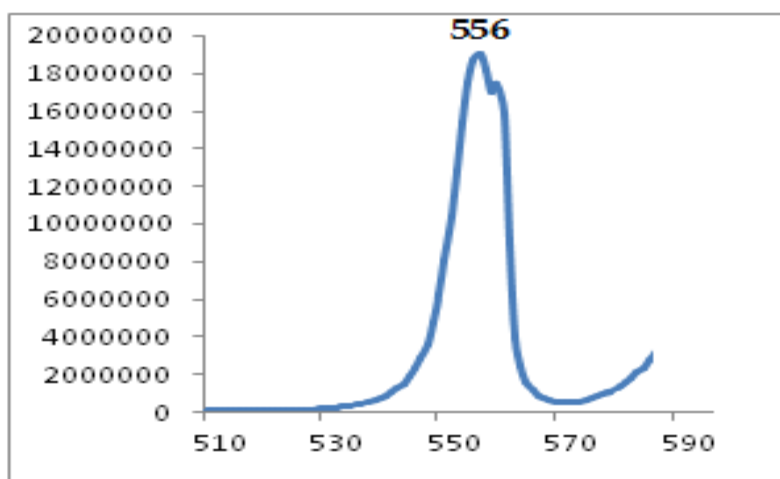


Figure 9: Fluorescence Emission spectrum for Fluorescein in ammonium hydroxide.

Table 1: Data of Ag-NP & Fluorescein in ammonia solution:

Sl.no	Sample	Excitation wavelength (nm)	Emission wavelength (nm) ϵ max ($M^{-1} cm^{-1}$)	Stocks shift (nm)
1	Ag-NP	342	438(800550)	96
2	Fluorescein	490	556(189007)	66

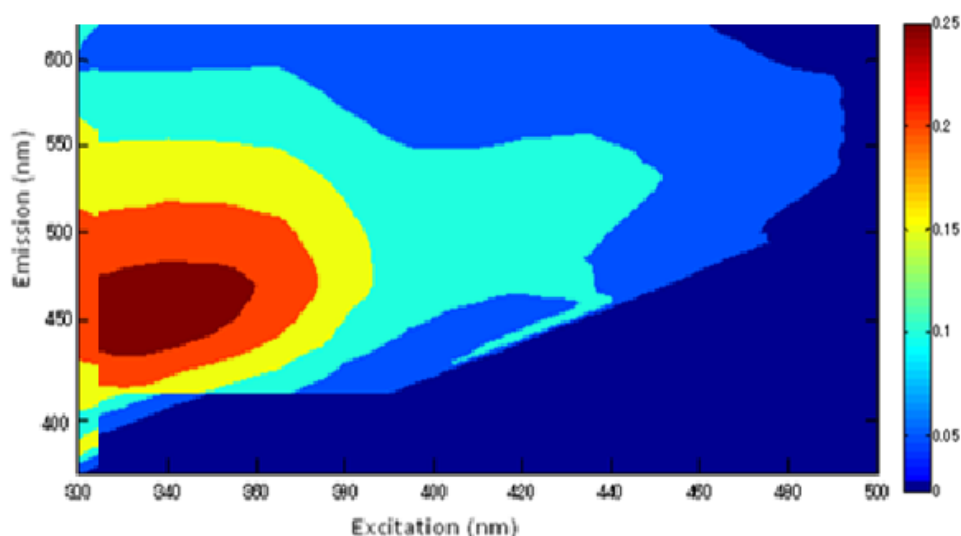


Figure 10: Excitation–emission matrices for Ag-NPs in ammonia solution. Location of the peak maxima: Ex. 342 nm/ Em438 nm, Fluorescence intensity in Raman units.

Table 2: Setup parameters for creation of EEMs

Parameter	
Scan Mode	Emission
Data Mode	Fluorescence
Excitation Wavelength Range (nm)	300 – 500
Excitation Step Invertval (nm)	5
Emission Wavelength Range (nm)	320 – 700
Emission Interval (nm)	5
Delay (s)	0
Excitation Shutter Opening (nm)	5
Emission Shutter Opening (nm)	5
PMT Voltage (V)	700
Response	Auto
Replicates	1
Shutter Control	ON
Spectrum Correction	ON

CONCLUSION

Plant extracted synthesis of silver nanoparticles is better than physico-chemical methods because it is eco-friendly, easy scale up of process ,While green biological methods which involve bacteria and fungi mediated synthesis of silver Nanoparticles requires a long time period. This plant extracted Synthesized silver nanoparticles were characterized by UV-Visible spectrophotometer, FTIR, XRD and TEM analysis. FT-IR provides information about functional groups which participates in the synthesis of silver nanoparticles. The interesting characteristic of silver nanoparticles is that they exhibit photoluminescence activity which is indicated by High stock's shift values.

References:

- [1] P. Mukherjee, A. Ahmad, D. Mandal, S. Senapati, S.R. Sainkar, M.I. Khan, R. Parishcha, P.V. Ajaykumar, M. Alam, R. Kumar, M. Sastry, *Nano Lett*, 2001, **1**, 515.
- [2] A. Ahmad, P. Mukherjee, D. Mandal, S. Senapati, M.I. Khan, R. Kumar, M. Sastry, *J. Am. Chem. Soc*, 2002, **124**, 12108.
- [3] M. Sastry, A. Ahmad, M.I. Khan, R. Kumar, *Curr. Sci*, 2003, **85**, 162.
- [4] S.S. Shankar, A. Ahmad, M. Sastry, *Biotechnol. Prog*, 2003, **19**, 1627.

- [5] S.S. Shankar, A. Rai, B. Ankamwar, A. Singh, A. Ahmad, M. Sastry, *Nat. Mater*, 2004, **3**, 482.
- [6] A. Rai, A. Singh, A. Ahmad, M. Sastry, *Langmuir*, 2006, **22**, 736.
- [7] J.L. Gardea-Torresdey, J.G. Parsons, K. Dokken, J.R. Peralta-Videa, H. Troiani, P.Santiago, M. Jose-Yacaman, *Nano Lett.* 2002, **2**, 397.
- [8] J.L. Gardea-Torresdey, E. Gomez, J.R. Peralta-Videa, J.G. Parsons, H. Troiani, M. Jose- Yacaman, *Langmuir*, 2003, **19**, 1357.
- [9] Kamat PV, *J Phys Chem B*, 2002, **106**, 7729.
- [10] Lakowicz J. R, Radiative decay engineering. *Anal Biochem*, 2001, **298**, 1.
- [11] Lakowicz J. R, Shen Y, D'Auria S, Malicka J, Fang J, Gryczynski Z, Gryczynski I, *Anal Biochem*, 2002, **301**, 261.
- [12] Lakowicz J. R, *Anal Biochem*, 2004, **324**, 153.
- [13] Aslan K, Gryczynski I, Malicka J, Lakowicz J. R, Geddes C. D, *Curr Opin Biotechnol*, 2005, **16(1)**, 55.
- [14] Aslan K, Holley P, Davies L, Lakowicz J. R, Geddes C. D, *J Am Chem Soc*, 2005, **127**, 12115.
- [15] Aslan K, Malyn S. N, Geddes C. D, *J Fluoresc*, 2007, **17**, 7.
- [16] Zhang J, Matveeva E, Gryczynski I, Leonenko Z, Lakowicz J. R, *J Phys Chem B* 2005, **109**, 7969.
- [17] Zhang J, Malicka J, Gryczynski I, Lakowicz J. R, *J Phys Chem B*, 2005, **109**, 7643.
- [18] Corrigan T. D, Guo S, Phaneuf R. J, Szmecinski H, *J Fluoresc*, 2005, **15**, 777.
- [19] Haes A. J, Stuart D. A, Nie S, Van Duyne R. P, *J Fluoresc*, 2004, **14**, 355.